

Multiphoton transitions between energy levels in a phase-biased Cooper-pair box

V.I. Shnyrkov,^{1,2} Th. Wagner,³ D. Born,¹ S.N. Shevchenko,² W. Krech,¹ A.N. Omelyanchouk,² E. Il'ichev,³ and H.-G. Meyer³

¹*Friedrich Schiller University, Institute of Solid State Physics, Helmholtzweg 5, D-07743 Jena, Germany*

²*B.Verkin Institute for Low Temperature Physics and Engineering of the National Academy of Sciences of Ukraine, 47 Lenin Ave., Kharkov 61103, Ukraine*

³*Institute for Physical High Technology, P.O. Box 100239, D-07702 Jena, Germany*

(Dated: October 6, 2018)

We investigated both theoretically and experimentally dynamic features of a phase-biased charge qubit consisting of a single-Cooper-pair transistor closed by a superconducting loop. The effective inductance of the qubit was probed by a high-quality tank circuit. In the presence of a microwave power, with a frequency of the order of the qubit energy level separation, an alteration of the qubit inductance was observed. We demonstrate that this effect is caused by the redistribution of the qubit level population. The excitation of the qubit by one-, two-, and three-photon processes was detected. Quantitative agreement between theory and experimental data was found.

PACS numbers: 74.50.+r, 85.25.Am, 85.25.Cp

I. INTRODUCTION

During the last decade a number of proposals for constructing an artificial quantum two-level system by making use of mesoscopic Josephson junctions were implemented^{1,2,3,4,5}. Since it was recognized that these circuits might serve as quantum bits (qubits) for quantum information devices the field has attracted increased attention.

Basically, two kinds of such devices have been developed, based on the charge or flux degree of freedom. Here we will consider one realization only, which is based on the charge degree of freedom. In this quantum system two charge states differing by $2e$ (e is the electron charge) are mixed by Josephson tunneling. One example of such a device is the single-Cooper-pair transistor - two mesoscopic tunnel junctions separated by a small superconducting island on which the charge can be induced by an external gate voltage⁶. The relative energy of the states is controlled by the gate voltage.

Since the measurement of a quantum system is a very delicate procedure, the readout sensor is a crucial component of any potential quantum computing circuit. In order to minimize the exchange of energy between detector and qubit the control of the reactive component of the output signals has been proposed and implemented⁷. Such kinds of measurements requires the proper design of the qubit. For instance a charge qubit can be a conventional single-Cooper-pair transistor closed by a superconducting loop⁸. For a certain range of the relationship between effective Josephson coupling and charge energies ε_J/E_C of the transistor's junctions, this device is effectively a two-level quantum system with externally controlled parameters^{6,8,9,10}. Moreover, similar to both the traditional nonhysteretic RF SQUID^{11,12} and the DC SQUID¹³, the phase-biased transistor coupled to a high-quality radio-frequency tank circuit¹⁴ turns out to be an ideal parametric converter of charge and flux signals with standard quantum limit of the energy resolution.

Recently measurements of the energy level separation of a superconducting charge qubit were reported. The qubit was coupled to a high quality tank circuit¹⁵ or non-resonantly to a single mode of the electromagnetic field of a superconducting on-chip resonator^{16,17}. Multiphoton transitions between energy levels in superconducting devices were studied in several articles^{18,19,20,21,22}; in this work we present both the experimental observation and the theoretical description of the multiphoton transitions between the ground and the first excited state in the phase-biased charge qubit^{6,8,9,10} making use of the impedance measurement technique^{23,24}.

We begin in Sec. II with a theoretical description of the phase-biased charge qubit (PBCQ) subjected to a time-dependent gate voltage or magnetic flux. We calculate the population of the upper level of this effective two-level system. The expression for the expectation value of the current in the PBCQ as well as the response of the tank circuit, weakly coupled to a PBCQ, have also been obtained. In Sec. III we describe the samples fabrication and the measurement setup. Comparison between theory and experimental data is discussed in the Sec. IV.

II. THEORY

A. Interaction of a phase-biased charge qubit with microwave power

The phase-biased charge qubit (PBCQ), schematically shown in Fig. 1, consists of two Josephson junctions closed by a superconducting ring. The charge en of the island between the junctions is controlled by the gate voltage V_g via the capacitance C_g , namely by the parameter $n_g = C_g V_g / e$; en_g is the polarization charge on the island. The junctions are characterized by the Josephson energies E_{J1} , E_{J2} and the phase differences δ_1 , δ_2 . The relevant energy values are the island's Coulomb energy, $E_C = e^2 / 2C_{tot}$, where C_{tot} is the total capac-

itance of the island, and the effective Josephson energy $\varepsilon_J = (E_{J1}^2 + E_{J2}^2 + 2E_{J1}E_{J2} \cos \delta)^{1/2}$. An important feature of the qubit is that its Josephson energy can be controlled by the external magnetic flux Φ_e piercing the ring. In this paper, the ring inductance L is assumed to be small. Consequently, the total phase difference, $\delta = \delta_1 + \delta_2$, is approximately equal to $\delta_e = 2\pi\Phi_e/\Phi_0$.

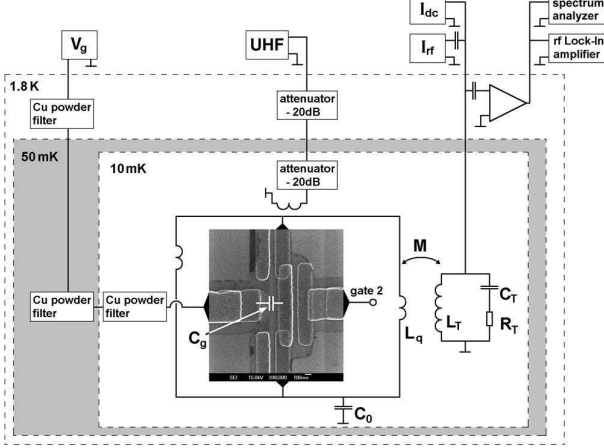


FIG. 1: Scheme of the PBCQ

The PBCQ is characterized by the Hamiltonian⁶:

$$H = 4E_C(n - n_g/2)^2 - E_{J1} \cos \delta_1 - E_{J2} \cos \delta_2, \quad (1)$$

which after quantization results in the following Hamiltonian, written in the representation based on the eigenstates of the operator \hat{n} , that is in the basis of the charge states $|n\rangle$:

$$\begin{aligned} \hat{H} = & \sum_n 4E_C(n - n_g/2)^2 |n\rangle \langle n| + \\ & + \frac{A}{2} \sum_n (|n+1\rangle \langle n| + |n-1\rangle \langle n|) + \\ & + \frac{B}{2i} \sum_n (|n+1\rangle \langle n| - |n-1\rangle \langle n|), \end{aligned} \quad (2)$$

$$A = -(E_{J1} + E_{J2}) \cos \frac{\delta}{2}, \quad B = -(E_{J1} - E_{J2}) \sin \frac{\delta}{2}. \quad (3)$$

This Hamiltonian in the two-level approximation can be rewritten in the basis of the charge states $\{|1\rangle, |0\rangle\}$ ⁹:

$$\hat{H} = \frac{A}{2} \hat{\tau}_x + \frac{B}{2} \hat{\tau}_y + \frac{C}{2} \hat{\tau}_z, \quad (4)$$

where the irrelevant term containing the unity matrix was omitted;

$$C = 4E_C(1 - n_g), \quad (5)$$

and $\hat{\tau}_i$ are the Pauli matrices: $\hat{\tau}_z |1\rangle = |1\rangle$, $\hat{\tau}_z |0\rangle = -|0\rangle$.

We consider two possibilities for the excitation of a PBCQ: (a) via gate voltage:

$$n_g(t) = n_g + \tilde{n}_g \sin \omega t, \quad \delta = \text{const}, \quad (6)$$

and (b) via magnetic flux:

$$\delta(t) = \delta_0 + \tilde{\delta} \sin \omega t, \quad n_g = \text{const}. \quad (7)$$

We shall consider first the time-independent case (which we denote by the subscript “0”). The eigenstates of the time-independent Hamiltonian

$$\hat{H}_0 = \frac{A_0}{2} \hat{\tau}_x + \frac{B_0}{2} \hat{\tau}_y + \frac{C_0}{2} \hat{\tau}_z, \quad (8)$$

denoted by $\{|-\rangle, |+\rangle\}$, are related to the charge states $\{|0\rangle, |1\rangle\}$ by the relation:

$$\begin{bmatrix} |-\rangle \\ |+\rangle \end{bmatrix} = \hat{S} \begin{bmatrix} |0\rangle \\ |1\rangle \end{bmatrix}. \quad (9)$$

Here

$$\hat{S} = \begin{bmatrix} \cos \frac{\eta}{2} & e^{i\psi} \sin \frac{\eta}{2} \\ -e^{-i\psi} \sin \frac{\eta}{2} & \cos \frac{\eta}{2} \end{bmatrix}, \quad (10)$$

where the mixing angles η , ψ are given by:

$$\sin \eta = \varepsilon_J / \Delta E, \quad \cos \eta = C_0 / \Delta E, \quad (11)$$

$$\sin \psi = B_0 / \varepsilon_J, \quad \cos \psi = -A_0 / \varepsilon_J \quad (12)$$

with

$$\varepsilon_J = \sqrt{A_0^2 + B_0^2}, \quad (13)$$

$$\begin{aligned} \Delta E &= \Delta E(n_g, \delta_0) = \sqrt{C_0^2 + \varepsilon_J^2} = \\ &= \sqrt{[4E_C(1 - n_g)]^2 + E_{J1}^2 + E_{J2}^2 + 2E_{J1}E_{J2} \cos \delta_0}. \end{aligned} \quad (14)$$

The diagonalization results in a Hamiltonian in the eigenstate basis:

$$\hat{H}'_0 = \hat{S}^{-1} \hat{H}_0 \hat{S} = \frac{\Delta E}{2} \hat{\sigma}_z, \quad (15)$$

where we denote the Pauli matrices, which operate in the eigenstate basis, by $\hat{\sigma}_i$, so that we have $\hat{\sigma}_z |+\rangle = |+\rangle$, $\hat{\sigma}_z |-\rangle = -|-\rangle$.

In order to get the probabilities of the system to be in the eigenstates of the stationary Hamiltonian \hat{H}_0 , we rewrite the time-dependent Hamiltonian $\hat{H}(t)$ in this basis. This Hamiltonian will be used in Sec. IV to solve the Bloch-type equation (the master equation) for the density matrix, whose diagonal elements define these probabilities²⁵.

We can split the Hamiltonian $\hat{H}(t)$ into two parts:

$$\hat{H}(t) = \hat{H}_0 + \hat{H}_1(t), \quad (16)$$

which gives:

$$\hat{H}'(t) = \hat{S}^{-1}\hat{H}(t)\hat{S} = \frac{\Delta E}{2}\hat{\sigma}_z + \hat{S}^{-1}\hat{H}_1(t)\hat{S}. \quad (17)$$

We consider first case (a), where the gate voltage is the time-dependent parameter as in Eq.(6). From Eq. (17) it follows:

$$\begin{aligned} \hat{H}'_a(t) &= \frac{\Delta E}{2}\hat{\sigma}_z - 2E_C\tilde{n}_g \sin \omega t \times \\ &\times [\cos \eta \cdot \hat{\sigma}_z - \sin \eta \sin \psi \cdot \hat{\sigma}_y + \sin \eta \cos \psi \cdot \hat{\sigma}_x]. \end{aligned} \quad (18)$$

We consider now case (b), where the magnetic flux is the time-dependent parameter, as in Eq. (7). In this case the time-dependent Hamiltonian (16) can be rewritten by expanding the quantities A and B in a Fourier series. However, we are interested only in small time-dependent perturbations and for the description of the experimental results we restrict ourselves to this case, when $\delta_0 = \pi$, $\tilde{\delta}/2 \ll \pi$. In the second approximation in $\tilde{\delta}$ the Hamiltonian can be written as

$$\begin{aligned} \hat{H}'_b(t) &= \frac{\Delta E}{2}\hat{\sigma}_z + (E_{J1} + E_{J2})\frac{\tilde{\delta}}{4}\sin \omega t \cdot \hat{\sigma}_x + \\ &+ (E_{J1} - E_{J2})\frac{\tilde{\delta}^2}{32}\cos 2\omega t \cdot \left\{ \frac{\varepsilon_J}{\Delta E}\hat{\sigma}_z - \frac{C}{\Delta E}\hat{\sigma}_y \right\}. \end{aligned} \quad (19)$$

B. Qubit-tank circuit arrangement

The current in a qubit ring is probed by the tank circuit, which is weakly coupled through a mutual inductance M to the PBCQ^{23,24}. The PBCQ is characterized by the inductance $L_{PBCQ} = L + L_J$, where L is the ring's inductance and L_J is an inductance defined by $L_J^{-1} = (2e/\hbar)\partial I/\partial \delta$. The effect of this inductance on the tank circuit can be represented by an effective inductance: $L_T \rightarrow L_{eff} = L_T + M^2/L_{PBCQ}$ (where M is the mutual inductance)²³.

The experimentally measurable value is the phase shift between the voltage and current in the tank circuit α . The expression for the phase shift at the resonant frequency $\omega_T = 1/\sqrt{L_T C_T}$ is (see e.g. in Ref. [26]):

$$\tan \alpha \simeq k^2 Q \cdot \frac{L}{L_J}, \quad (20)$$

Here $Q^{-1} = \omega_T C_T R_T$, $k^2 = M^2/(L \cdot L_T)$, and we have neglected the ring's inductance L in the denominator. Thus the phase shift α is defined by L_J , i.e. by the current-phase relation $I(\delta)$. This can be used to define the current-phase dependence in Josephson junctions^{23,27}. In the quantum case the current is equal to the expectation value of the current operator: $I =$

$\langle \hat{I} \rangle$. For our system we have^{6,9}: $\hat{I} = -I_0 \hat{\sigma}_z$, where the ground state current is

$$I_0 = \frac{e}{\hbar} E_{J1} E_{J2} \frac{\sin \delta}{\Delta E}. \quad (21)$$

Thus, $I = I_0 Z$, where $Z = \langle \hat{\sigma}_z \rangle = Sp(\hat{\rho} \hat{\sigma}_z)$, and $\hat{\rho}$ is the reduced density matrix. This means that the current flows with the probability P_+ in one direction and with the probability $P_- = 1 - P_+$ in the other direction; and the introduced value Z is equal to $Z = 1 - 2P_+$. Thus from Eq. (20) for the time-averaged phase shift α we have:

$$\tan \alpha \simeq k^2 Q \cdot \frac{2e}{\hbar} L \cdot \left\{ \frac{\partial I_0}{\partial \delta} \cdot \bar{Z} + I_0 \cdot \frac{\partial \bar{Z}}{\partial \delta} \right\}, \quad (22)$$

where the bar stands for the time-averaging. We note that for a weakly driven system the function $\bar{P}_+(\omega, \delta, n_g)$ has the maxima (resonant peaks) at $\Delta E(\delta, n_g) = K \cdot \hbar \omega$ (K is an integer) and, consequently, its derivative (see Eq. (22)) has hyperbolic-like behavior.

In the particular case, when $\delta = \pi$ we have $I_0 = 0$ and from Eq. (22) it follows:

$$\tan \alpha \simeq -\lambda \cdot \left(\frac{\Delta E}{E_C} \right)^{-1} \cdot (1 - 2\bar{P}_+), \quad (23)$$

$$\lambda = k^2 Q \cdot \frac{2e^2 L E_C}{\hbar^2} \cdot \frac{E_{J1} E_{J2}}{E_C^2}. \quad (24)$$

This means that the dependence of α on n_g at $\delta = \pi$ contains resonances at $\Delta E(n_g) = K \cdot \hbar \omega$.

III. SAMPLE PREPARATION AND MEASUREMENTS

A SEM image of the gradiometer-type charge qubit's core with two closely spaced mesoscopic Josephson junctions is shown along with the electrical circuitry in Fig. 1. The junction areas are slightly larger than 100×100 nm² leading to critical currents I_C of 50–100 nA, which can be estimated from the measured tunnel resistances. The Cooper-box charge (on the island between the Josephson junctions) can be continuously varied by the gate voltage. Both the junctions and the island are imbedded in a macroscopic (0.5×1 mm²) superconducting gradiometer-type-loop, which was done in order to minimize vibration and magnetic noise. The single-Cooper-pair transistor and the loop were fabricated by e-beam lithography and shadow evaporation of aluminum. One loop of the gradiometer is inductively coupled by a flip-chip configuration to the niobium high quality tank coil.

We study the ‘‘qubit + tank’’ impedance as a function of the polarization charge en_g and the phase difference δ , by making use of a well-known impedance measurement technique. The tank circuit is driven by an rf current I_{rf}

of frequency ω_T close to the resonance frequency of the tank circuit. The phase difference α of the tank voltage (with respect to the phase of the applied current I_{rf}) is measured as a function of the gate voltage $V_g = V_g(n_g)$ and of the external magnetic flux $\Phi_e = \Phi_e(\delta)$. These measurements show a shift in the resonant frequency of the “qubit + tank” arrangement due to a change in the effective inductance of the sample. The tank voltage was sequentially amplified by means of a cryogenic rf preamplifier, a room temperature amplifier, and further relevant standard electronics.

The measurements were carried out in a dilution-type refrigerator at a nominal temperature of about 10 mK. In order to minimize the noise level inherent in the total gate voltage, we equipped the transistor’s gate line (a ThermoCoax between 2 K and 10 mK) with conventional low-pass RC and microwave copper powder filters (Fig. 1). For an efficient thermalization of the charge gate, three microwave filters were mounted on different low-temperature plates (2 K, 50 mK, and 10 mK) of the refrigerator. The power attenuation of these 10 cm long filters was determined as a function of the frequency (up to 45 GHz) at room temperature. From the measurement results, we concluded that the total attenuation of this line was more than 80 dB in the GHz range. A high-attenuation ThermoCoax line along with two (on the 2 K and 10 mK) cooled commercial 20 dB-attenuators were used for applying a microwave power (“UHF gate”) to the sample. This microwave line is coupled inductively to the Pb-shield resonance cavity with the qubit inside. At the microwave frequency the current fed into the Pb shield is amplified by the quality factor of the resonator, producing an electromagnetic field. In our measurements special care was taken to avoid the magnetic coupling between the microwave line and the qubit: (i) the qubit sample was placed across a Pb resonator for maximum electric (E)-field interaction and (ii) the gradiometer-type topology of the qubit circuit prevents the sample from the interaction via mutual inductance with the microwave line. As a further evidence for E-coupling via the length of the Al thin film charge-gate electrode, only the noise-like output signal on microwave power was obtained with sample after mechanical break of this thin film gate line.

By passing a dc bias current through the tank coil (Fig. 1) we could simply control the flux-induced currents circulating in the qubit ring, because of the mutual inductance between qubit and tank. For the tank, we prepared square-shaped Nb pancake coils on oxidized Si substrates²⁸. For flexibility, only the coil was made lithographically. We use an external capacitance C_T to be able to change the resonance frequency of the tank which, in this particular case was 28.9 MHz. The tank circuit was coupled by a 30 cm long piece of two-wire line to the cold HEMT-amplifier. Changes of the phase of the tank voltage oscillations due to variations of the Josephson inductance of the sample were measured by means of an averaging procedure: every measurement point was taken (with a time constant of 0.1 ms) 50 times and av-

eraged. Cryogenic μ -metal and superconducting shields protected the sample against external magnetic and electric noises. However, we could not take any special action to avoid the drift of electrostatic carriers within the substrate, so the $1/f$ noise due to background charge motion is not completely negligible in our experiments.

IV. RESULTS AND DISCUSSION

A. Analysis of the experimental results

The dependence of the phase shift α on the gate voltage is shown in Figs. 2a and 3a. In the first set of experiments, we used different frequencies of the microwave excitation at a nominally fixed power (see Fig. 2a). In a similar manner to the results reported before¹⁵ the $\alpha(n_g)$ dependence exhibits clear peaks. Their positions depend on the frequency of excitation. Recently it was shown, that the peaks are due to resonant excitations of the system from ground to upper states¹⁵. In the obtained dependencies a second set of the peaks is clearly seen (the grey arrows in Fig. 2). These “additional” peaks would be due to two-photon excitation. In order to clarify this issue we fixed the frequency of the excitation and measured $\alpha(n_g)$ for different microwave powers. Indeed, as was expected, the “additional” peak structure becomes clearer for higher powers (see Fig. 3a). Moreover, an additional structure appears in the $\alpha(\Phi_e)$ dependence as well (see Fig. 5a).

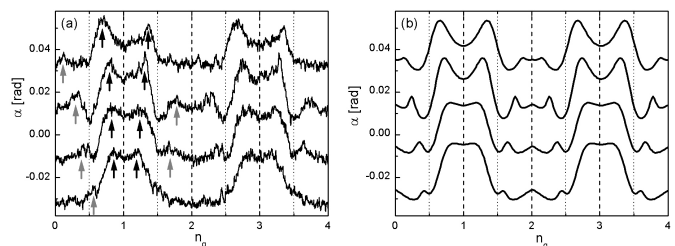


FIG. 2: Resonant excitation of the PBCQ: dependence of the phase shift α on the time-independent part of the dimensionless gate voltage n_g at $\delta = \pi$. The curves correspond to a fixed power of excitation in experiment (a) and an amplitude $\tilde{n}_g \simeq 0.3$ in theory (b). The varied parameter is the frequency $\omega/2\pi$, which from the bottom to top curves is: 6.5, 7.1, 8.1, 9.1 GHz. Upper curves are shifted vertically for clarity. Black (grey) arrows show the one- (two-) photon resonances.

Let us extract the value of the minimum energy level separation $\Delta E_{\min} = E_{J1} - E_{J2}$ from the experimental results. In order to do that we define the position of the resonances, marked with the arrows in Fig. 2a: they correspond to $\Delta E(n_g) = K \cdot \hbar\omega$. We put these points in the $n_g - \Delta E$ -plane: see Fig. 4, where the circles and squares correspond to one- and two-photon resonances, respectively, for which $K = 1, 2$. The fitting of these data

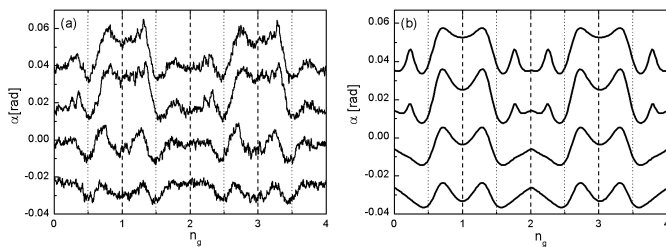


FIG. 3: The same as in Fig. 2 but at a fixed frequency $\omega/2\pi = 8.2$ GHz with the varied parameter: in experiment (a) being power of excitation (from bottom to top: -75, -63, -49, -42 (dB)) and in theory (b) being amplitude \tilde{n}_g (from bottom to top: 0.1, 0.2, 0.3, 0.4). Upper curves are shifted.

with the expression

$$\Delta E(n_g, \delta = \pi) = \sqrt{[4E_C(1 - n_g)]^2 + (E_{J1} - E_{J2})^2} \quad (25)$$

allows us to estimate both E_C and $\Delta E_{\min} = \Delta E(n_g = 1, \delta = \pi) = E_{J1} - E_{J2}$ (see Fig. 4).

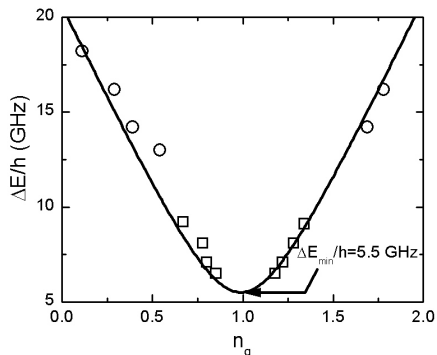


FIG. 4: Energy level separation ΔE as a function of n_g at $\delta = \pi$. Squares and circles correspond to one- and two-photon resonances; solid line is a fit with $E_C/h = 5$ GHz and $\Delta E_{\min}/h = (E_{J1} - E_{J2})/h = 5.5$ GHz.

B. Numerical calculations

In this subsection we present the results of the quantitative description of the system. In order to obtain the dependence of the tank voltage phase shift α on the system's parameters we made use of Eqs. (22) and (23). The probability that the upper level is occupied, $P_+(t)$, was obtained from the solution of the master equation for the density matrix as described in Ref.²⁵. In order to take into account the relaxation and dephasing processes the corresponding rates Γ_{relax} and Γ_ϕ are included in the master equation phenomenologically²⁹. We note that the numerical solution of the master equation is the general approach used to describe the nonlinear

dynamic behavior of a two-level system subjected to an external field of arbitrary amplitude and frequency (see in²⁵ and references therein). When the amplitude of the field is small and its frequency is close to the energy level separation divided by an integer, the analytical consideration, known as the rotating-wave approximation, can be applied to the description of the multiphoton transitions (see e.g.³⁰). The latter approach was developed for the description of the PBCQ both analytically³¹ and numerically³².

In order to unify expressions (18) and (19) and to get the equations needed for numerical calculations, we write down the Hamiltonian \hat{H}' as follows:

$$\hat{H}' \equiv \frac{R}{2}\hat{\sigma}_x + \frac{S}{2}\hat{\sigma}_y + \frac{T}{2}\hat{\sigma}_z. \quad (26)$$

Consequently, the evolution of the reduced density matrix $\hat{\rho}$ taken in the form

$$\hat{\rho} = \frac{1}{2} \begin{bmatrix} 1 + Z & X - iY \\ X + iY & 1 - Z \end{bmatrix}, \quad (27)$$

is described by the master equation in the form of Bloch equations (see in^{25,29}):

$$\frac{dX}{dt} = \frac{S}{\hbar}Z - \frac{T}{\hbar}Y - \Gamma_\phi X, \quad (28)$$

$$\frac{dY}{dt} = -\frac{R}{\hbar}Z + \frac{T}{\hbar}X - \Gamma_\phi Y, \quad (29)$$

$$\frac{dZ}{dt} = \frac{R}{\hbar}Y - \frac{S}{\hbar}X - \Gamma_{relax}(Z - Z(0)). \quad (30)$$

From these equations we get $Z(t)$ which defines the occupation probability of the upper level $|+\rangle$, $P_+(t) = \rho_{22}(t) = \frac{1}{2}(1 - Z(t))$. We choose the initial condition to be $X(0) = Y(0) = 0$, $Z(0) = 1$, which corresponds to the system being in the ground state $|-\rangle$.

Quantitative analysis with Eqs. (19) and (28)-(30) has shown that the case when the magnetic flux is time-dependent (Eq. (7)) is not consistent with the experimental results presented in this work. By that we have confirmed the argument, presented in Sec. III, that the qubit mainly is not excited via the magnetic flux, but rather via the gate voltage. So in what follows we will consider the case when the time-dependent parameter is the gate voltage (Eq. (6)). Then the system is described by the Hamiltonian of Eq. (18).

We consider first the dependence of the phase shift α on n_g at $\delta = \pi$. The results of the numerical calculation are shown in Figs. 2b and 3b. In order to fit the experimental curves, by making use of Eqs. (23) and (28)-(30), we have taken: $\Gamma_\phi/(E_C/h) \sim 0.3$ and $\Gamma_{relax}/(E_C/h) \sim 0.05$ (which corresponds to the following decoherence and relaxation times: $T_\phi = \Gamma_\phi^{-1} \simeq 0.7ns$ and $T_{relax} = \Gamma_{relax}^{-1} \simeq 4ns$) and $\lambda = 0.1$. This value of λ is in good agreement with the value estimated from Eq. (24) for the system's parameters experimentally accessible. The relaxation and decoherence rates were assumed

to be independent of the system's parameters for simplicity. We note that the shape of the curves, in particular the widths and the heights of the resonances, is defined by three parameters: amplitude (\tilde{n}_g) and the relaxation and decoherence rates. These values can be determined from the analysis of the widths and the heights of the resonances as e.g. in Ref.²¹. But we rather fit the whole curves, which allows us to determine the system's parameters.

Now we consider the dependence of the phase shift α on δ by making use of Eqs. (22) and (28)-(30): see Fig. 5. From the above considerations we have the following parameters: λ , E_C and $E_{J1} - E_{J2}$. But at $\delta \neq \pi$ we also need $E_{J1,2}$ (see Eq.(22)). At $\delta \neq \pi$ in the $\alpha - \delta$ -curve, due to the domination of the second term in Eq. (22), the multiphoton resonances result in the hyperbolic-like behaviour with $\alpha \simeq 0$ at $\Delta E = K\hbar\omega$. We note that in the vicinity of $\delta = \pi$ the first term in Eq. (22) decreases the value of α , which explains why the one-photon hyperbolic-like excitation is not symmetric about $\alpha = 0$ axis. From the position of these points, marked with the arrows in Fig. 5a (namely from the relation $\Delta E(n_g, \delta) = K\hbar\omega$, see Eq. (14)), we found: $E_{J1}/h \simeq 8E_C/h = 40$ GHz, $E_{J2}/h \simeq 6.9E_C/h = 34.5$ GHz, and also $n_g \simeq 0.85$. With these values we have calculated the dependence of α on δ , shown in Fig. 5b. To fit the experimental curves we have taken: $\Gamma_\phi/(E_C/h) = 0.05$ and $\Gamma_{relax}/(E_C/h) = 0.03$, which correspond to the following decoherence and relaxation times: $T_\phi = \Gamma_\phi^{-1} \simeq 4ns$ and $T_{relax} = \Gamma_{relax}^{-1} \simeq 7ns$.

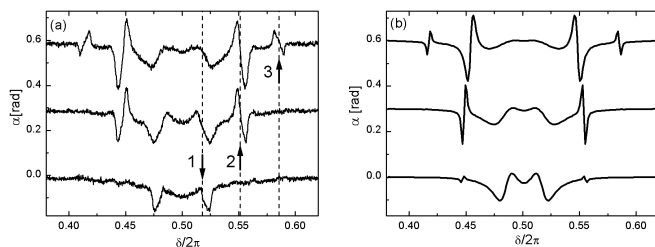


FIG. 5: Dependence of the tank voltage phase shift α on the phase difference δ . The curves correspond to the fixed frequency $\omega/2\pi = 7.05$ GHz with the varied parameter: in experiment (a) being power of excitation (from bottom to top: -80, -60, -57 (dB)) and in theory (b) being amplitude \tilde{n}_g (from bottom to top: 0.1, 0.2, 0.4). Upper curves are shifted. The arrows show the appearance of 1-, 2-, and 3-photon excitations at $\Delta E(\delta) = K\hbar\omega$, $K = 1, 2, 3$.

V. CONCLUSIONS

Multiphoton (namely, one-, two-, and three-photon) excitations of the PBCQ were observed experimentally and described theoretically. The multiphoton transitions manifest themselves in the dependence of the tank voltage phase shift α on the qubit's parameters as follows: there are resonances in the dependence of α on n_g at $\delta = \pi$ and there are hyperbolic-like dips and peaks in the dependence of α on δ . Theoretical fitting has allowed us to find out the qubit's parameters, particularly the relaxation and decoherence rates, which characterize the decoherence processes in the system.

Acknowledgments

The authors would like to thank D. Averin and Ya. S. Greenberg for fruitful discussions. V.I.Sh. acknowledges the financial support of the Deutsche Forschungsgemeinschaft under grant No. KR1172/9-2. E.I. thanks the EU for support through the RSFQubit project. A.N.O. and S.N.Sh. acknowledge the grant "Nanosystems, nanomaterials, and nanotechnology" of the National Academy of Sciences of Ukraine.

- ¹ Y. Nakamura, Yu. A. Pashkin, and J.S. Tsai, *Nature* **398**, 786 (1999).
- ² J.R. Friedman, V. Patel, W. Chen, S.K. Tolpygo, and J.E. Lukens, *Nature* **406**, 43 (2000).
- ³ C.H. van der Wal, A.C.J. ter Haar, F.K. Wilhelm, R.N. Schouten, C.J.P.M. Harmans, T.P. Orlando, S. Lloyd, and J.E. Mooij, *Science* **290**, 773 (2000).
- ⁴ D. Vion, A. Aassime, A. Cottet, P. Joyez, H. Pothier, C. Urbina, D. Esteve, and M.H. Devoret, *Science* **296**, 886 (2002).
- ⁵ I. Chiorescu, Y. Nakamura, C.J.P.M. Harmans, and J.E. Mooij, *Science* **299**, 1869 (2002).
- ⁶ M. Tinkham, *Introduction to Superconductivity*, Chapter 7, 2nd edition, Mc Graw-Hill, New York (1996).
- ⁷ E. Il'ichev, N. Oukhanski, Th. Wagner, H.-G. Meyer, A.Yu. Smirnov, M. Grajcar, A. Izmalkov, D.Born, W. Krech, and

- A. Zagoskin, *Low Temp. Phys.* **30**, 620 (2004).
- ⁸ J.R. Friedman and D.V. Averin, *Phys. Rev. Lett.* **88**, 050403 (2002).
- ⁹ W. Krech, M. Grajcar, D. Born, I. Zhilyaev, Th. Wagner, E. Il'ichev, Ya. Greenberg, *Phys. Lett. A* **303**, 352 (2002).
- ¹⁰ A.B. Zorin, *Physica C* **368**, 284 (2002).
- ¹¹ V.V. Danilov and K.K. Likharev, *Sov. Jour. Tech. Phys.* **XLV**, 1110 (1975).
- ¹² I.M. Dmitrenko, G.M. Tsoi, V.I. Shnyrkov, V.V. Kartsovnik, *J. Low Temp. Phys.* **49**, 417 (1982); V.I. Shnyrkov, V.A. Khlus, and G.M. Tsoi, *J. Low Temp. Phys.* **39**, 477 (1980).
- ¹³ M. Mück, J.B. Kycia, and J. Clarke, *Appl. Phys. Lett.* **78**, 967 (2001).
- ¹⁴ A.B. Zorin, *Phys. Rev. Lett.* **86**, 3388 (2001).
- ¹⁵ D. Born, V.I. Shnyrkov, W. Krech, Th. Wagner, E. Il'ichev,

- M. Grajcar, U. Hübner, and H.-G. Meyer, Phys. Rev. **B70**, 180501(R) (2004).
- ¹⁶ A. Wallraff, D. I. Schuster, A. Blais, L. Frunzio, R.-S. Huang, J. Majer, S. Kumar, S. M. Girvin, R. J. Schoelkopf, Nature (London) **431**, 162, (2004).
- ¹⁷ D. I. Schuster, A. Wallraff, A. Blais, L. Frunzio, R.-S. Huang, J. Majer, S. M. Girvin, R. J. Schoelkopf, Phys. Rev. Lett. **94**, 123602 (2005).
- ¹⁸ Y. Nakamura, Yu. A. Pashkin, and J.S. Tsai, Phys. Rev. Lett. **87**, 246601 (2001).
- ¹⁹ A. Wallraff, T. Duty, A. Lukashenko, A.V. Ustinov, Phys. Rev. Lett. **90**, 037003 (2003).
- ²⁰ J.Q. You and F. Nori, Phys. Rev. B **68**, 064509 (2003).
- ²¹ S. Saito, M. Thorwart, H. Tanaka, M. Ueda, H. Nakano, K. Semba, and H. Takayanagi, Phys. Rev. Lett. **93**, 037001 (2004).
- ²² Yu-xi Liu, L.F. Wei, and F. Nori, Phys. Rev. A **71**, 063820 (2005).
- ²³ R. Rifkin and B.S. Deaver, Jr., Phys. Rev. B **13**, 3894 (1976).
- ²⁴ E. Il'ichev, V. Zakosarenko, L. Fritzsche, R. Stolz, H.E. Hoenig, H.-G. Meyer, M. Götz, A.B. Zorin, V.V. Khanin, A.B. Pavolotsky, and J. Niemeyer, Rev. Sci. Instr. **72**, 1882 (2001).
- ²⁵ S.N. Shevchenko, A.S. Kiyko, A.N. Omelyanchouk, W. Krech, Low Temp. Phys. **31**, 569 (2005) [Fiz. Nizk. Temp. **31**, 752 (2005)].
- ²⁶ L.D. Landau, E.M. Lifshitz, *Electrodynamics of Continuous Media*, paragraph 62, 2nd edition, Moscow, Nauka (1982) (in Russian).
- ²⁷ A.A. Golubov, M.Yu. Kupriyanov, E. Il'ichev, Rev. Mod. Phys. **76**, 411 (2004).
- ²⁸ T. May, E. Il'ichev, M. Grajcar, H.-G. Meyer, Rev. Sci. Instr. **74**, 1282 (2003).
- ²⁹ K. Blum, *Density Matrix Theory and Applications*, Plenum Press, New York–London (1981).
- ³⁰ C. Cohen-Tannoudji, J. Dupont-Roc, and G. Grynberg, *Atom-Photon Interactions*, Wiley, New York (1992).
- ³¹ W. Krech, D. Born, V. Shnyrkov, Th. Wagner, M. Grajcar, E. Il'ichev, H.-G. Meyer, Ya. Greenberg, IEEE Trans. Appl. Supercond. **15**, 876 (2005).
- ³² M. Amft, Master thesis, Friedrich Schiller University, Jena (2005).